J. Biochem. 121, 1139-1146 (1997)

Spectroscopic Studies of Rat Liver Acyl-CoA Oxidase with Reference to Recognition and Activation of Substrate[1]

Haruhiko Tamaoki,* Chiaki Setoyama,* Retsu Miura,*,[2] Iwaho Hazekawa,† Yasuzo Nishina,† and Kiyoshi Shiga†

*Departments of *Biochemistry and †Physiology, Kumamoto University School of Medicine, 2-2-1 Honjo, Kumamoto 860*

Received for publication, February 5, 1997

Two forms of rat peroxisomal acyl-CoA oxidase (ACO-I and -II) interact with the substrate analogs, 3-ketoacyl-CoAs, forming a complex characterized by the so-called charge-transfer (CT) band around 575 nm in the absorption spectra. The CT band of ACO-I exhibited a broad dependency on the acyl chain-length from C4 to C16, whereas that of ACO-II showed increased intensity with a longer acyl chain to reach a maximum with a chain-length of C12. These chain-length dependencies of the CT bands were compared with those of the enzymatic activities reported previously [Setoyama *et al.* (1995) *Biochem. Biophys. Res. Commun.* 217, 482-487]. The differences in spectroscopic and enzymatic properties between ACO-I and -II suggest that the amino acid stretch corresponding to the third exon in the ACO sequence affects the binding of the ligand and substrate, since the difference in the primary structure between ACO-I and -II lies in the short amino acid stretch corresponding to the third of the total of 14 exons. On the other hand, resonance Raman spectra of the complexes of ACO-I and -II with 3-ketoacyl-CoAs excited in the CT band showed similar features. The two prominent FAD bands II and III, associated with the C(4*a*)=N(5) moiety of FAD, were observed at 1,577 and 1,545 cm^{-1}, respectively. In contrast, the bands at 1,615 and 1,493 cm^{-1} in the ACO-I·3-keto-C8-CoA complex were assigned to the stretching modes of C=O at positions 3 and 1 of the ligand, respectively, by using the isotopically labeled ligands. Both C=O stretching bands were shifted to lower wave numbers upon complex formation with ACO-I, implying that the C=O bond involves the single bond (C-O^-) character in the active site cavity. The downshift of the C(1)=O stretching band was larger than that of the C(3)=O stretching band. Therefore, the ligand lies in the active site as the anionic form with a major contribution from C(1)-O^-. These observations demonstrate that the CT band around 575 nm arises from the charge-transfer interaction between the oxidized FAD and the enolate transformed after the elimination of the α-proton. The band II of FAD in the complexes reveals a significant decrease in the frequency in comparison with the complexes of medium-chain acyl-CoA dehydrogenase (MCAD) with 3-ketoacyl-CoA. This observation suggests a difference between ACO and MCAD in the hydrogen-bonding network associated with enzyme-bound FAD.

Key words: acyl-CoA dehydrogenase, acyl-CoA oxidase, charge-transfer interaction, flavoenzyme, resonance Raman spectra.

In mammalian cells, fatty acids are oxidized through two major systems, namely, the mitochondrial and peroxisomal β-oxidation systems (*1-3*). Acyl-CoA oxidase [EC 1.3.3.6] (ACO), which is the first and rate-limiting enzyme in the peroxisomal β-oxidation pathway, catalyzes the H_2O_2-generating dehydrogenation of acyl-CoA thioesters to the corresponding *trans*-2-enoyl-CoA thioesters. ACO constitutes a superfamily with acyl-CoA dehydrogenase (ACD), the first enzyme in the mitochondrial β-oxidation system (*4*). Osumi *et al.* (*5*) have reported purification of ACO from the rat liver and its molecular and enzymatic properties. The expression system using insect cells provided preparations of rat and human ACO with high efficiency (*6, 7*).

Recent studies on the structures of the ACO gene revealed that two forms of ACO mRNA (ACO-I and -II) are produced by alternative splicing in the rat liver (*8, 9*). The difference between ACO-I and -II is localized only in the third of the total of 14 exons, which corresponds to residues 90-143 of the total of 661 amino acids (*3, 8*). ACO-I and -II exhibit 55 and 50% identities in this region at the nucleotide

[1] This study is supported in part by a Grant-in-Aid for Scientific Research (No. 07458160) from the Ministry of Education, Science, Sports and Culture of Japan and by a Research Grant from the Japan Society for the Promotion of Science (Research for the Future).

[2] To whom correspondence shoud be addressed. Phone: +81-96-373-5062, FAX: +81-96-373-5066, E-mail: miura@gpo.kumamoto-u.ac.jp

Abbreviations: ACO, acyl-CoA oxidase; ACD, acyl-CoA dehydrogenase; MCAD, medium-chain acyl-CoA dehydrogenase; 3-keto-CX-CoA, straight-chain 3-ketoacyl-CoA, where X denotes the carbon number of 3-ketoacyl chain.

and amino acid levels, respectively (*3, 8*). The ratio of the rat ACO-I and -II seems to be regulated transcriptionally during peroxisome proliferation and also in a tissue-specific fashion (*10*). Moreover, analysis of the organization of the human ACO gene suggested the presence of two forms of ACO mRNA (*11*). We separately prepared the two forms of rat ACO using an expression system in *Escherichia coli*, and subsequently investigated their enzyme activities and substrate specificities (*12*). The purified enzymes showed different substrate specificities from each other: ACO-I exhibited optimum activities toward acyl-CoAs with shorter acyl chains in comparison with ACO-II. Our results indicate that the occurrence of the two forms of ACO may be physiologically significant in the metabolic regulation of the fatty acids.

In the ACO reaction, a glutamate residue, which is conserved in ACDs (*13*), is responsible for the abstraction of the α-proton of a substrate acyl-CoA (*13*). The ACO reaction, therefore, is regarded as being initiated by the α-proton abstraction by a glutamate residue in concert with the β-hydride transfer to flavin. Our interest is focused on the mechanisms by which a substrate is recognized and activated in the catalytic event. To understand these mechanisms at a submolecular level, we studied the interaction of ACO with a series of 3-ketoacyl-CoAs as substrate analogs by means of electronic absorption and resonance Raman spectroscopy. The oxidized form of ACO-I or -II forms a complex with 3-ketoacyl-CoA, exhibiting a broad absorption band in the long wavelength region, which is characteristic of charge-transfer complexes observed in many flavoenzymes as catalytic intermediates or as enzyme-ligand complexes (*14*). The results obtained herein will be discussed in relation to the enzymatic activities and to the difference between ACO-I and -II.

MATERIALS AND METHODS

Rat liver ACO-I and -II were prepared using a pET expression system in *E. coli* BL21(DE3) cells as previously reported (*12*). The concentrations of ACO-I and -II were estimated using molar extinction coefficients of $\varepsilon_{445}=12.6\pm0.1$ and $\varepsilon_{448}=12.3\pm0.1$ $mM^{-1}\cdot cm^{-1}$, respectively, which were determined by the method of Thorpe *et al.* (*15*) (see "RESULTS"). MCAD was purified from pig kidney as described elsewhere (*16, 17*). Catalase, crotonase, and β-hydroxyacyl-CoA dehydrogenase were obtained from Sigma, USA. Other chemicals were of the highest grade available from commercial sources and used as supplied.

3-Ketoacyl-CoAs other than 3-keto-C16-CoA were prepared in three steps (*18*). First, saturated acyl-CoAs with acyl chain-lengths of C4-C12 were synthesized from corresponding fatty acids by the method of Kawaguchi *et al.* (*19*); these were converted to *trans*-2,3-enoyl CoAs by incubation in the presence of MCAD, catalase and 1-methylphenazinium methyl sulfate (*18*); and finally, *trans*-2,3-enoyl-CoAs were transformed to 3-ketoacyl-CoAs by incubation with crotonase and β-hydroxyacyl-CoA dehydrogenase (*20*). 3-Keto-C16-CoA was prepared by the method of Thorpe (*21*). 3-Ketoacyl-CoAs thus prepared were purified by HPLC, then desalted by chromatography on a Sephadex G-10 (Pharmacia) column with water (*18*). All purified derivatives were stored at -80°C as lyophilized powders. Purity of samples was confirmed by HPLC just before use. The concentration of 3-ketoacyl-CoA was estimated using a molar extinction coefficient of 16 $mM^{-1}\cdot cm^{-1}$ (*22*). The isotopically labeled 3-keto-C8-CoA was synthesized with C8 fatty acid that was labeled with ^{13}C at the carboxyl carbon (99 atom% enriched, Isotec, USA). $H_2{}^{18}O$ (97.9 atom% enriched, Isotec, USA) was used to replace the oxygen at C(3)=O of 3-keto-C8-CoA with $C(3)={}^{18}O$ (*18, 23*).

The absorption and Raman spectra were measured in 50 mM potassium phosphate buffer, pH 7.4, at about 25°C with a Hitachi U-3210 spectrometer and a JASCO NR-1800 spectrometer, respectively. The resonance Raman spectra were performed with excitation at 632.8 nm using a He-Ne Laser (NEC GLG5900). The Raman spectra were calibrated with indene.

RESULTS

Electronic Spectra of ACO—The extinction coefficients of ACO were determined according to the method of Thorpe *et al.* (*15*), using ACO-I and -II preparations from which unbound FAD had been removed by repeated dialysis. Enzyme-bound FAD in 50 mM potassium phosphate, pH 7.4, was released by adding three volumes of 8.0 M guanidine hydrochloride, 50 mM potassium phosphate, pH 7.4. The resultant absorbance was compared with that of free FAD solution prepared under the same conditions. On the basis of ε_{450} of 11.3 $mM^{-1}\cdot cm^{-1}$ for FAD in the phosphate buffer, the absorbance of ACO-I and -II solutions was scaled as extinction coefficient on the ordinate. Figure 1 shows the average spectra of three experiments for ACO-I, -II, and free FAD. The extinction coefficients of the first flavin band for ACO-I and -II were calculated to be $\varepsilon_{445}=12.6\pm0.1$ and $\varepsilon_{448}=12.3\pm0.1$ $mM^{-1}\cdot cm^{-1}$, respectively. These extinction coefficients are about 20% lower than that of pig MCAD, $\varepsilon_{445}=15.4$ $mM^{-1}\cdot cm^{-1}$ (*15*). Among other flavoenzyme oxidases, *e.g.*, glucose oxidase ($\varepsilon_{450}=14.1$ $mM^{-1}\cdot cm^{-1}$) (*24*), pyruvate oxidase ($\varepsilon_{460}=12.7$ $mM^{-1}\cdot cm^{-1}$) (*25*) and D-amino acid oxidase ($\varepsilon_{445}=11.3$ $mM^{-1}\cdot cm^{-1}$) (*26*), ACOs show intermediate values for the corresponding coefficient. Figure 1 also displays the substantial difference between the two enzymes in the second band for FAD

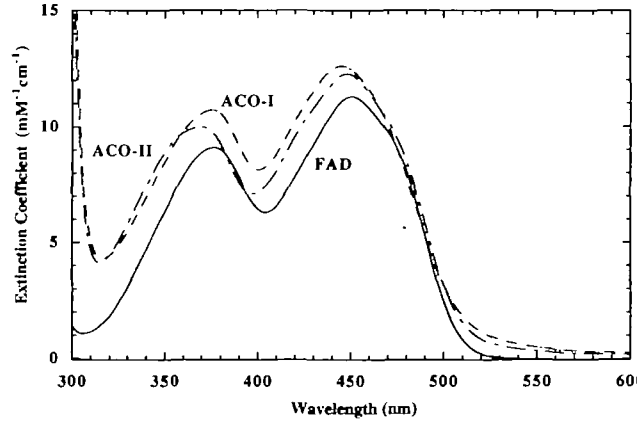

Fig. 1. **Absorption spectra of ACO and FAD.** ACO-I (dotted line), ACO-II (dotted-dotted line) and FAD (solid line). The ordinate represents the extinction coefficient. ACO-I, -II, and FAD were used in the range of 9.42–67.2 μM.

around 370 nm, whose extinction coefficients were calculated to be 10.8±0.1 (376 nm) and 10.0±0.1 $mM^{-1} \cdot cm^{-1}$ (370 nm) for ACO-I and -II, respectively.

Interaction of ACO-I with Acetoacetyl-CoA—Figure 2 demonstrates the spectrophotometric titration of ACO-I with acetoacetyl-CoA. The concentrations of ACO-I were fixed at 43.0 μM in all spectra. A new broad absorption band was observed in the long wavelength region. As will be discussed later, the new absorption is related to the charge-transfer (CT) from the anionic form of acetoacetyl-CoA to the oxidized FAD. This peculiar absorption band is therefore referred to as a charge-transfer (CT) band hereafter. With the increase of the CT band, the FAD absorption centered at 445 nm decreased. Difference spectra in Fig. 2B clearly show the CT band with its maximum at 575 nm and the minimum at 478 nm for the first FAD absorption band. The FAD absorption around 370 nm was practically unaltered.

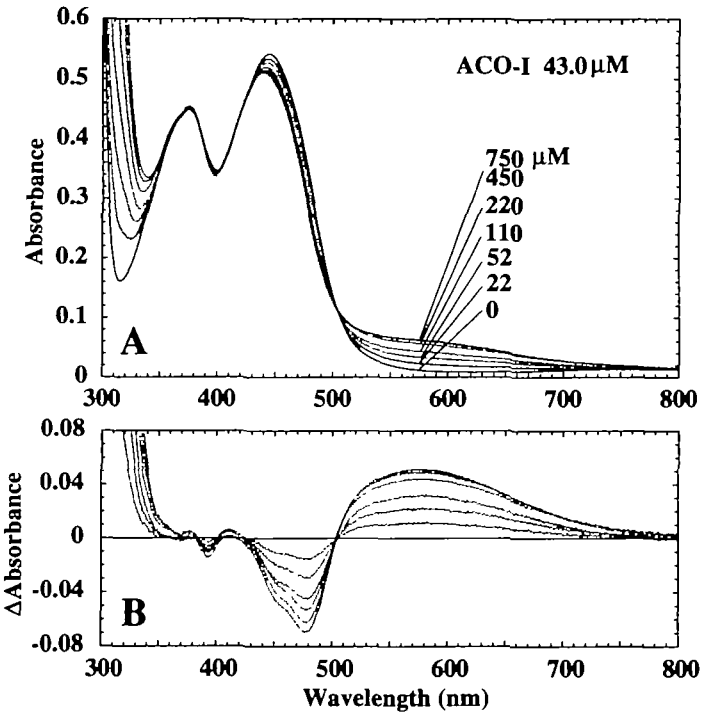

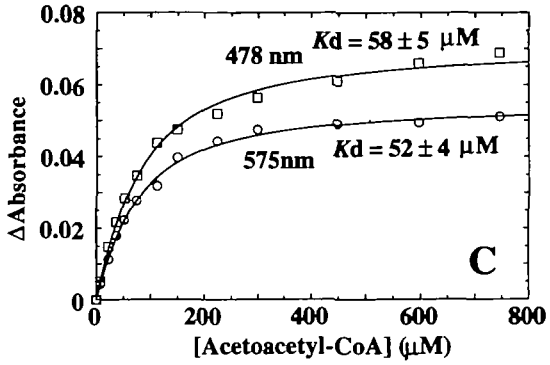

Fig. 2. **Spectral titration of ACO-I with acetoacetyl-CoA.** (A) ACO-I, 43.0 μM, (solid line) was titrated with acetoacetyl-CoA. The concentration of acetoacetyl-CoA was varied from 22 to 750 μM (dotted lines). (B) Difference spectra (complexed minus uncomplexed) of ACO-I. (C) Plots of the intensities at 575 (circles) and 478 nm (squares) against the concentration of acetoacetyl-CoA, with the theoretical curves (solid lines) fitted for a two-state equilibrium with the dissociation constant as parameter.

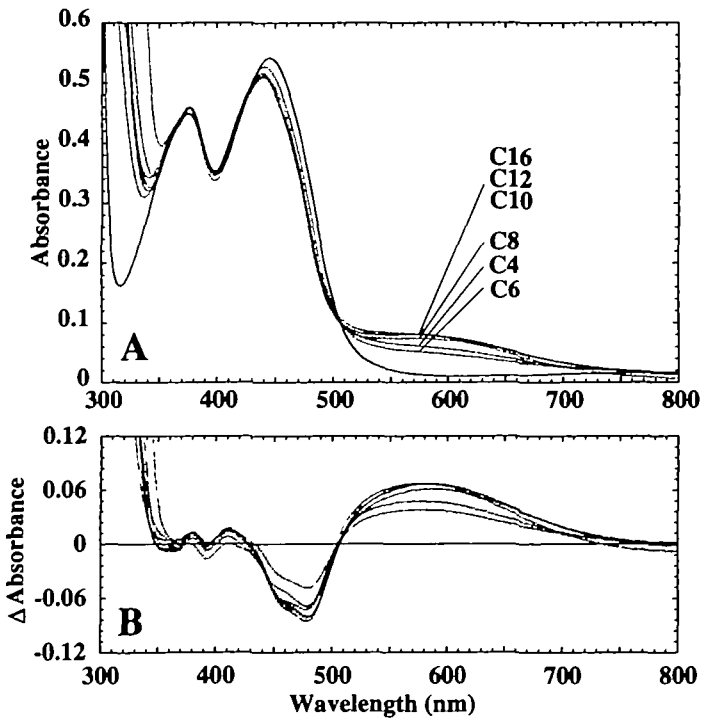

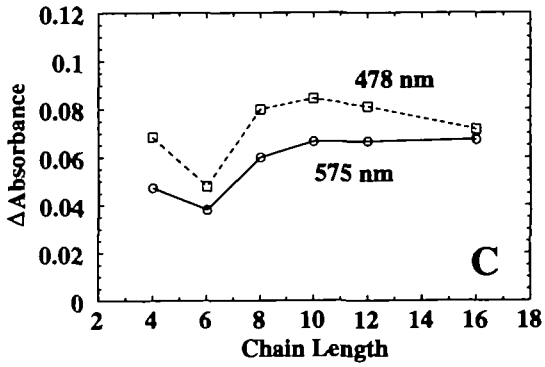

Fig. 3. **Absorption spectra of the complexes of ACO-I with different 3-ketoacyl-CoAs.** (A) ACO-I (solid line) was complexed with 3-ketoacyl-CoAs with acyl chains of C4-C16 (dotted lines). (B) Difference spectra (complexed minus uncomplexed) of ACO-I. (C) Plots of the intensities at 575 (circles) and 478 nm (squares) against acyl chain-length. Concentrations were: ACO-I, 43.0 μM; acetoacetyl-CoA, 0.75 mM; 3-keto-C6-CoA, 0.80 mM; 3-keto-C8-CoA, 0.83 mM; 3-keto-C10-CoA, 0.83 mM; 3-keto-C12-CoA, 0.87 mM; 3-keto-C16-CoA, 0.75 mM.

The isosbestic point at 504 nm reveals that the complex formation of ACO-I with acetoacetyl-CoA is a two-state process. From the plots of the absorbances at 575 and 478 nm against the ligand concentration (Fig. 2C), the dissociation constants, K_ds, were evaluated to be 52 ± 4 and 58 ± 5 μM, respectively. These values seemed essentially identical and are larger than that of pig MCAD with acetoacetyl-CoA [12 μM (*27*) or 12.6 ± 0.9 μM (*28*)]. The differences in molar extinction coefficient between the complexed and the free ACO-I were found to be 1.28 ± 0.02 and 1.66 ± 0.03 $mM^{-1}\cdot cm^{-1}$ at 575 and 478 nm, respectively. For ACO-I the maximal extinction coefficient change for the CT band is smaller than that of pig MCAD, 3.3 $mM^{-1}\cdot cm^{-1}$ at 545 nm (*27*). The maximum of the CT band of ACO-I is red-shifted by 30 nm from that of MCAD. The extinction coefficients of the complex were estimated to be $\varepsilon_{575}=1.58\pm0.02$ and $\varepsilon_{440}=11.9\pm0.1$ $mM^{-1}\cdot cm^{-1}$.

Absorption Spectra of the Complexes of ACO with Various 3-Ketoacyl-CoAs—The spectral changes of ACO upon complex formation with various 3-ketoacyl-CoAs are shown in Figs. 3 and 4. The absorption spectra were measured under conditions where the enzyme was saturated with each ligand.

The difference spectra in Fig. 3B are quite similar to one another, even though ACO-I was complexed with different ligands. And the difference spectra cross the zero line at nearly the same wavelength of 505 nm. This feature closely resembles that observed in the interaction of ACO-I with acetoacetyl-CoA (Fig. 2). Although we have not yet found a plausible explanation for this spectral resemblance, it might come from the similar binding mode of ACO with 3-ketoacyl-CoAs examined. The absorbances at 575 and 478 nm were plotted as a function of the number of carbon atoms in the acyl chain (Fig. 3C). The profile of acyl chain-length dependency shows a broad pattern, and the maximum appeared at acyl chain-length of C8-C16. On the other hand, the profile of the spectral changes of ACO-II upon complex formation shows a different pattern with respect to the acyl chain-length specificity, the magnitude of the CT band being greater at longer chain-lengths, as shown in Fig. 4. The profiles of the intensities at 575 and 478 nm reached the maximum at the acyl chain-length of C12 (Fig. 4C). The most distinct difference from ACO-I was observed at about 387 nm, which results from the shift and increase of the second FAD absorption band by the complex formation. The chain-length dependency observed at 387 nm coincides with those observed at 575 and 478 nm. The difference spectra share a common crossing point at 499 nm with the zero line.

As mentioned above, the spectral changes of the ACO complexes, including the CT-band strength, depend on the acyl chain-length of 3-ketoacyl-CoA; and the chain-length dependency is distinctly different between ACO-I and -II. The complexes of ACO-I and -II with 3-ketoacyl-CoAs also showed a subtle difference in the CT-band shape and a remarkable difference in the second FAD absorption at 370 nm, suggesting that the binding mode of the ligands is slightly different between the two enzymes.

Resonance Raman Spectra of the ACO·3-Ketoacyl-CoA Complexes—Resonance Raman spectra of the complexes were measured with excitation at 632.8 nm, which is within the CT band of the complexes. The complexes of ACO-I·3-keto-C8-CoA and ACO-II·3-keto-C16-CoA show similar spectral features to each other (Fig. 5). The prominent bands at 1,577 and 1,545 cm^{-1} [bands II and III, respectively according to the nomenclature of Bowman and Spiro (*29*)] in the ACO complexes correspond to those observed in the complexes of beef MCAD with 3-ketoacyl-CoAs; and these bands can be associated with the C(4*a*)=N(5) moiety of FAD (Fig. 6) on the basis of the similarity to the MCAD complexes (*18*). Band II in ACO complexes (1,577 cm^{-1}) revealed a small but significant decrease in frequency in

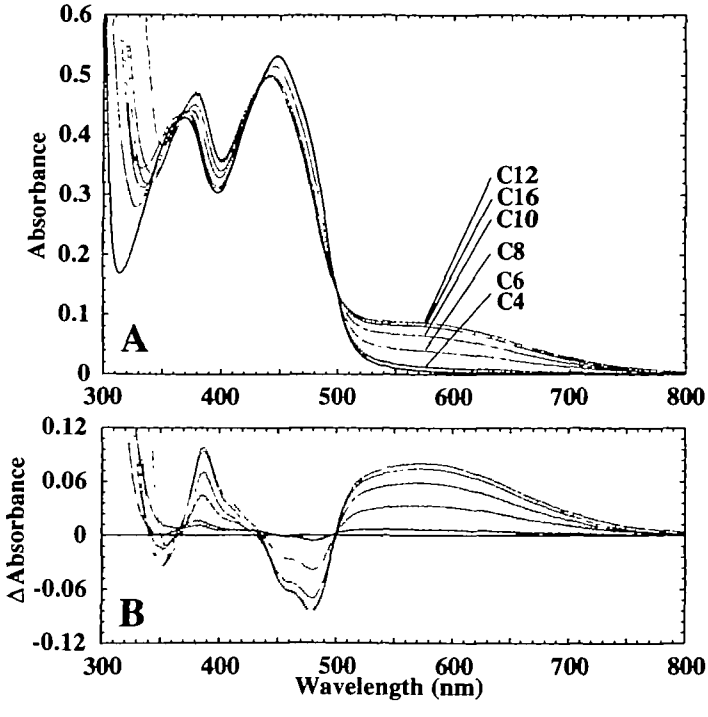

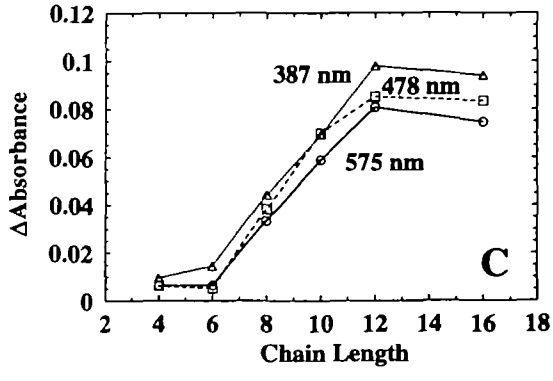

Fig. 4. **Absorption spectra of the complexes of ACO-II with different 3-ketoacyl-CoAs.** (A) ACO-II (solid line) was complexed with 3-ketoacyl-CoAs with acyl chains of C4-C16 (dotted lines). (B) Difference spectra (complexed minus uncomplexed) of ACO-II. (C) Plots of the intensities at 575 (circles), 478 (squares), and 387 nm (triangles) against acyl chain-length. Concentration of ACO-II was 43.3 μM and concentrations of 3-ketoacyl-CoAs were the same as those described in Fig. 3.

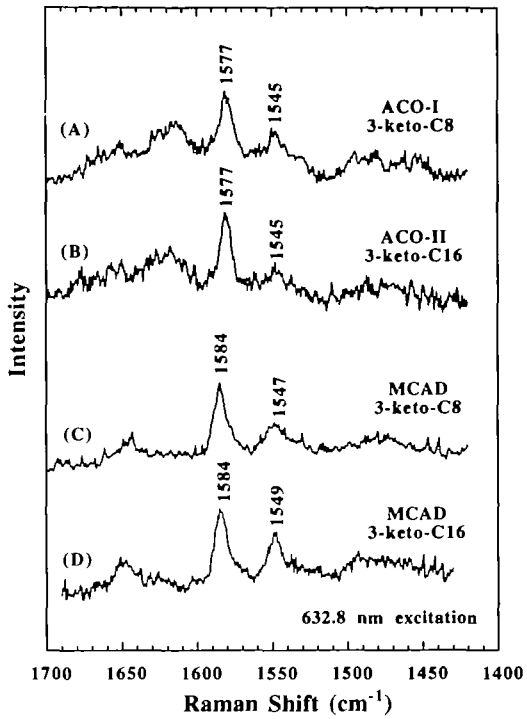

Fig. 5. **Resonance Raman spectra, excited at 632.8 nm, of the complexes of ACO·3-ketoacyl-CoAs.** The spectra of MCAD·3-ketoacyl-CoAs are shown for comparison (*18*).(A) ACO-I·3-keto-C8-CoA. (B) ACO-II·3-keto-C16-CoA. (C) MCAD·3-keto-C8-CoA. (D) MCAD·3-keto-C16-CoA. Concentrations were: (A) ACO-I, 1.8 mM; 3-keto-C8-CoA, 2.2 mM. (B) ACO-II, 2.1 mM; 3-keto-C16-CoA, 3.1 mM. (C) MCAD, 1.1 mM; 3-keto-C8-CoA, 1.4 mM. (D) MCAD, 1.4 mM; 3-keto-C16-CoA, 1.7 mM.

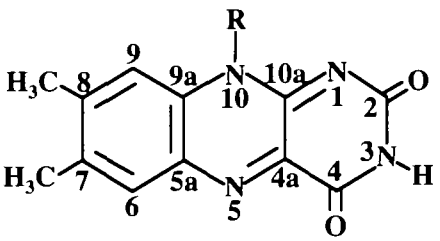

Fig. 6. **Numbering of the flavin ring system.**

comparison with the corresponding band in the MCAD complexes, which was reported by Hazekawa *et al.* (*ca.* 1,584 cm^{-1}, Fig. 5) (*18*). The difference in the frequency between ACO and MCAD complexes reflects the difference in the environments of FAD in the two enzymes, which may be caused by differences in the networks of hydrogen bonding around the flavin ring (*30, 31*) or in the alignment between FAD and the ligand.

The vibrational bands of the ligand were assigned by using the isotopically labeled 3-keto-C8-CoA, in which carbonyl oxygen and carbon were labeled with ^{18}O and ^{13}C at positions 3 and 1, respectively. Since the oxygen at C(3)=O is exchangeable with that of solvent water (*18, 23*), the enzyme solution was repeatedly concentrated and diluted using the buffer in $H_2{}^{18}O$. Finally, at least 90% of the oxygen at C(3)=O was exchanged for ^{18}O. As shown in Fig. 7, A and B, the band intensity around 1,615 cm^{-1} is

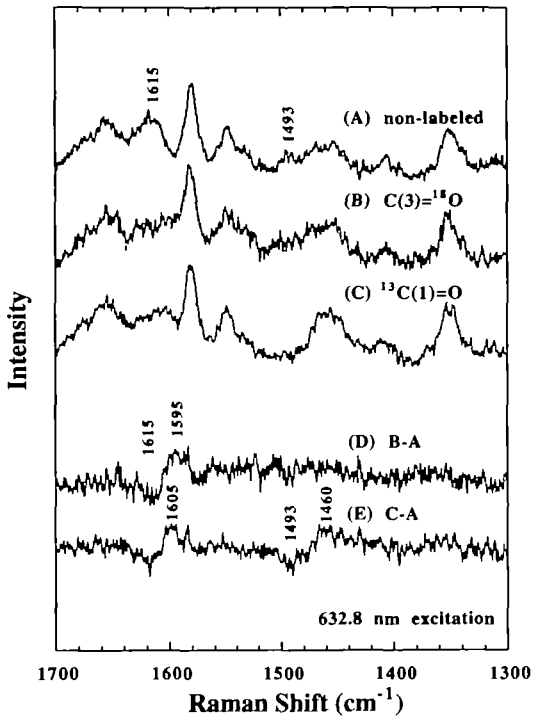

Fig. 7. **Resonance Raman spectra of ACO-I complexed with the isotopically labeled 3-keto-C8-CoAs.** (A) ACO-I, 2.4 mM; 3-keto-C8-CoA, 3.1 mM. (B) ACO-I, 1.6 mM; C(3)=^{18}O labeled 3-keto-C8-CoA, 2.0 mM. (C) ACO-I, 2.4 mM; ^{13}C-1 labeled 3-keto-C8-CoA, 3.3 mM. (D) Difference spectrum, B-A. (E) Difference spectrum, C-A.

decreased in the complex with the C(3)=^{18}O ligand in comparison with the complex with the unlabeled ligand. The difference spectrum (B-A) made it clear that the band shift by the isotope effect at C(3)=^{18}O was from 1,615 to 1,595 cm^{-1} and that the other bands were not significantly affected (Fig. 7D). Therefore, we assigned the 1,615-cm^{-1} band to the C(3)=O stretching mode.

In the spectrum of the complex with the ^{13}C(1)=O labeled ligand, the Raman band at 1,493 cm^{-1}, which was observed in the non-labeled (Fig. 7A) or ^{18}O-labeled ligand (Fig. 7B), disappeared and the broad band at about 1,460 cm^{-1} changed in shape and intensity. From the difference spectrum (C-A) in Fig. 7E, the 1,493-cm^{-1} band was shifted to 1,460 cm^{-1}, where it overlapped the broad band at 1,460 cm^{-1} (compare spectra C and E in Fig. 7). The band assigned to the C(3)=O stretching mode was shifted to 1,605 cm^{-1}, showing that the C(1)=O stretching mode also contributes to this band. In fact, acetoacetyl-CoA in the free form as well as in the bound form with ACDs exhibited similar isotope effects when the Raman spectra of the labeled ligand with ^{13}C(1)=O were measured (*18*). On the other hand, the 1,493-cm^{-1} band in Fig. 7A contained little contribution from the vibrational mode of C(3)=O stretching, since the spectral features around this band remained unchanged in the complex with the C(3)=^{18}O labeled ligand. The 1,493-cm^{-1} band was assigned to the C(1)=O stretching mode.

DISCUSSION

We observed the resonance Raman bands of the complexes

of ACO with 3-ketoacyl-CoAs upon the CT-band excitation. Among the enhanced Raman bands of the ACO-I•3-keto-C8-CoA and ACO-II•3-keto-C16-CoA complexes, the two prominent bands observed at 1,577 and 1,545 cm^{-1} were assigned to vibrational modes related to the C(4*a*)=N(5) region of FAD. The two bands at 1,493 and 1,615 cm^{-1} in the ACO•3-C8-CoA complex were assigned to the C(1)=O and C(3)=O stretching bands, respectively, with the isotopically labeled ligands. These C=O stretching bands of the bound ligand were shifted to lower frequencies in comparison with the free ligand. In free acetoacetyl-CoA, the corresponding C=O stretching bands were observed at 1,650 and 1,716 cm^{-1}, respectively (*18*), and the downshifts of the bound ligand were estimated to be 157 and 101 cm^{-1}, respectively. Similar downshifts were reported for the complexes of several kinds of ACDs with 3-ketoacyl-CoAs by Nishina *et al.* (*32*) and Hazekawa *et al.* (*18*). The C(1)=O and C(3)=O stretching bands were observed at 1,487 and 1,613 cm^{-1}, respectively, for the pig MCAD•acetoacetyl-CoA (*32*) and at 1,476 and 1,622 cm^{-1}, respectively, for the beef MCAD•acetoacetyl-CoA (*18*). From the ^{13}C NMR measurements, Miura *et al.* (*33*) demonstrated that acetoacetyl-CoA is complexed with pig MCAD as an enol(ate) form, in which the C(2) carbon takes the sp^2 configuration, indicating that one of the protons at C(2) is abstracted in the complexed state. Thorpe *et al.* (*27, 34*) postulated that the complex of MCAD with 3-ketoacyl-CoA is a charge-transfer complex between an enolate form of the ligand and the oxidized FAD.

As members of the same superfamily, ACO and ACD seem to catalyze the β-dehydrogenation reaction through similar processes in the reductive half-reaction (*1-3*). Sequence alignments of ACO with ACDs indicated a conserved glutamate residue, which is a catalytic base responsible for the α-proton abstraction of a substrate (*13*). The ACO reaction is expected to be initiated by the α-proton abstraction, and this abstraction step can be viewed as a common step in the process in the enzyme reaction and the complex formation with 3-ketoacyl-CoA. From the analogy of MCAD, we conclude that 3-ketoacyl-CoA occupies the active site as an anionic form, after the α-proton abstraction by a catalytic base. The α-proton abstraction transforms 3-ketoacyl-CoA to the anionic form, which can be expressed as the three canonical forms (two enolate forms and carboanionic form), as represented in Scheme 1. The downshifts of C=O stretching bands indicate that the bond of C=O involves the single bond (C-O^-)

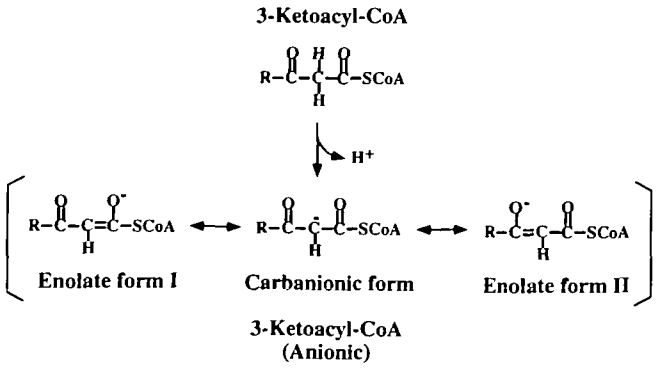

Scheme 1. **Neutral and anionic structures of 3-ketoacyl-CoA.**

character, namely, a contribution from enolate form I or II. The shifts of the bands for C(1)=O and C(3)=O further indicate that the ligand lies toward the enolate form I with C(1)-O^- polarization. Since Raman bands derived from both oxidized FAD and the ligand become resonance-enhanced when the CT band is excited, these band can be ascribed to the charge-transfer interaction between oxidized FAD and the anionic form of the ligand. In view of the electron-withdrawing nature of oxidized flavin and the electron-richness of the anionic form, the charge-transfer should be from the ligand to the oxidized form of flavin.

With regard to the complex of MCAD with the substrate, C8-CoA, Kim *et al.* (*35*) reported that the carbonyl oxygen of the substrate is hydrogen-bonded to the main-chain amide of Glu376 as well as to the ribityl 2′-hydroxyl group of FAD on the basis of the crystal structure. The polarization at the C(1)=O bond induced by these hydrogen bonds facilitates activation of the substrate by lowering the pK_a of the α-proton which is to be abstracted by Glu376 residue in the dehydrogenation step. As a similar hydrogen-bonding network is expected to participate in the oxidation reaction or the complex formation of ACO, our observation of the downshift of the band for C(1)=O stretching might reflect a similar mode of substrate activation. However, it is difficult to estimate the contribution of hydrogen bonding in the downshift of C(1)=O band separately from the contribution derived from an enolate form of the substrate or ligand.

In previous work (*12*), we compared the oxidase activities of ACO-I and -II and demonstrated that the two enzymes have different substrate specificities. Due to the lower values of critical micelle concentration for substrates with longer acyl chains (*36*), the kinetic parameter V_{max} or k_{cat} is not always easily estimated; and the relative activity for each substrate was therefore represented as the activity measured at a fixed concentration of 69 μM for each acyl-CoA (*12*). ACO-I shows the optimum activity at a shorter chain-length relative to ACO-II; the optimum activity of ACO-I was observed at the acyl chain-length of C10, whereas ACO-II exhibited the optimum at C14 under the conditions employed.

The spectral changes for ACO-I•3-ketoacyl-CoAs showed a broad pattern with a maximum in the range of C8-C16, whereas the chain-length dependency on the activity of ACO-I is maximum at a chain-length of C10 (*12*). On the other hand, the chain-length dependency on the spectral changes of ACO-II with 3-ketoacyl-CoAs coincides closely with that of its activities (*12*), which were very low with C4 and C6 acyl-CoAs and gradually increased with the longer acyl-CoAs to reach the maximum with C14 acyl-CoA.

Spectroscopic and activity measurements thus demonstrated that ACO-I and -II differ in chain-length dependencies. Moreover, the complexes of ACO-I and -II with 3-ketoacyl-CoAs showed the differences in the second FAD absorption at 370 nm and in the CT-band shape. An important implication with respect to the structural differences between ACO-I and -II is that the amino acid stretch, which corresponds to the third exon, affects the binding of the substrates and ligands. ACOs and ACDs are considered to have evolved from a common primordial gene and to belong to the same superfamily (*3, 4*). From the alignment of rat ACO with several acyl-CoA dehydrogenases (*4, 13*), the amino acid stretch that distinguishes one ACO from the

other corresponds to residues 86-140 of porcine MCAD. According to the crystal structure (*35*), this portion of MCAD indeed interacts with the substrate. This indicates that, in ACO, the amino acid stretch in question does influence the substrate binding. The spectral differences between ACO-I and -II and the differences observed in the enzyme activity may be derived from the divergence of the active site, which stems from the difference of the amino acid stretch corresponding to the third exon.

The activity observed for ACO is related to the process of oxidation of the substrate, the simultaneous reduction of the enzyme and reoxidation of the reduced enzyme. On the other hand, the spectral observation is derived from the complex formation between the oxidized ACO and the ligand. The two properties of the enzyme should therefore be distinguished one from the other. However, if the complex formation with the ligand shares a common step with an event in the catalytic process, comparison of the two properties should yield valuable information in terms of substrate recognition or substrate activation. As discussed above, the CT band originates from the charge-transfer interaction between the oxidized FAD as an acceptor and the anionic form of 3-ketoacyl-CoA, after abstraction of the α-proton, as a donor. The fact that the acyl chain-length dependencies of the two properties showed similar patterns seems to offer proof that the α-proton abstraction by the catalytic base is such common step.

The charge-transfer interaction is generally accomplished by the overlap between the lowest unoccupied molecular orbital of the acceptor and the highest occupied molecular orbital of the donor. The intensity and shape of the CT band, therefore, would be sensitive to change in the alignment of the two interacting species. However, we observed that the complexes of each ACO with 3-ketoacyl-CoAs of varying acyl chain-length gave similar absorption spectral features, though with different intensities. If the chain-length specificity of the ligand reflects the alignment of the ligand and FAD, one would expect the absorption spectrum of ACO complexed with a ligand to differ depending on the ligand. One explanation for our observation is that the variation in alignment of the two molecules with change in acyl chain-length is sufficient to perturb only the transition probability for the CT state. However, it is also possible to explain the observation by an equilibrium between the multiple orientations of the enzyme-ligand complex at the active site. With regard to the MCAD complexes with several kinds of substrates and ligands, the chain-length dependencies have been investigated by the electronic absorption spectra (*37*). Recently, Lee *et al.* (*38*) reported that the complexes of the double mutant of human MCAD (Glu376Gly/Thr255Glu) with the substrates possess two conformations, *i.e.*, "active" and "inactive" forms, of the enzyme and also multiple conformations of the substrate. Although the relation between enzyme and substrate conformations is not clear, the population ratio of "active" and "inactive" forms was altered by changing chain-length of the substrate (*38*). In an "inactive" form, the glutamate residue that is responsible for abstracting the α-proton of the substrate was hydrogen-bonded to another residue, resulting in an inactive, *i.e.*, abortive, enzyme-substrate complex. We can similarly suppose that two major alignments are possible between FAD and the ligand at the active site: an "active" alignment with an anionic ligand (CT complex) and an "inactive" alignment with a ligand (non-CT complex). The change in the ratio of "active" and "inactive" forms with change in the chain-length could provide an explanation for our observation. We are now conducting further spectroscopic and crystallographic studies to solve the questions raised herein and to elucidate the catalytic properties of ACO at a submolecular level.

REFERENCES

1. Schulz, H. (1991) Beta oxidation of fatty acids. *Biochim. Biophys. Acta* **1081**, 109-120
2. Osumi, T. (1993) Structure and expression of the genes encoding peroxisomal β-oxidation enzymes. *Biochimie* **75**, 243-250
3. Kunau, W.-H., Dommes, V., and Schulz, H. (1995) β-Oxidation of fatty acids in mitochondria, peroxisomes, and bacteria: A century of continued progress. *Prog. Lipid Res.* **34**, 267-342
4. Tanaka, K. and Indo, Y. (1992) Evolution of the acyl-CoA dehydrogenase/oxidase superfamily. *Prog. Clin. Biol. Res.* **375**, 95-110
5. Osumi, T., Hashimoto, T., and Ui, N. (1980) Purification and properties of acyl-CoA oxidase from rat liver. *J. Biochem.* **87**, 1735-1746
6. Chu, R., Usuda, N., Reddy, M.K., Liu, C., Hashimoto, T., Alvares, K., Rao, M.S., and Reddy, J.K. (1994) Functional expression of rat peroxisomal acyl-CoA oxidase in *Spodoptera frugiperda* cells. *Biochem. Biophys. Res. Commun.* **200**, 178-186
7. Chu, R., Varanasi, U., Chu, S., Lin, Y., Usuda, N., Rao, M.S., and Reddy, J.K. (1995) Overexpression and characterization of the human peroxisomal acyl-CoA oxidase in insect cells. *J. Biol. Chem.* **270**, 4908-4915
8. Miyazawa, S., Hayashi, H., Hijikata, M., Ishii, N., Furuta, S., Kagamiyama, H., Osumi, T., and Hashimoto, T. (1987) Complete nucleotide sequence of cDNA and predicted amino acid sequence of rat acyl-CoA oxidase. *J. Biol. Chem.* **262**, 8131-8137
9. Osumi, T., Ishii, N., Miyazawa, S., and Hashimoto, T. (1987) Isolation and structural characterization of the rat acyl-CoA oxidase gene. *J. Biol. Chem.* **262**, 8138-8143
10. Bell, D.R. and Elcombe, C.R. (1991) Regulation of differential spliced transcripts of acyl-CoA oxidase in the rat. *Biochim. Biophys. Acta* **1090**, 211-215
11. Varanasi, U., Chu, R., Chu, S., Espinosa, R., LeBeau, M.M., and Reddy, J.K. (1994) Isolation of the human peroxisomal acyl-CoA oxidase gene: Organization, promoter analysis, and chromosomal localization. *Proc. Natl. Acad. Sci. USA* **91**, 3107-3111
12. Setoyama, C., Tamaoki, H., Nishina, Y., Shiga, K., and Miura, R. (1995) Functional expression of two forms of rat acyl-CoA oxidase and their substrate specificities. *Biochem. Biophys. Res. Commun.* **217**, 482-487
13. Matsubara, Y., Indo, Y., Naito, E., Ozasa, H., Glassberg, R., Vockley, J., Ikeda, Y., Kraus, J., and Tanaka, K. (1989) Molecular cloning and nucleotide sequence of cDNAs encoding the precursors of rat long chain acyl-coenzyme A, short chain acyl-coenzyme A, and isovaleryl-coenzyme A dehydrogenases. *J. Biol. Chem.* **264**, 16321-16331
14. Massey, V. and Ghisla, S. (1974) Role of charge-transfer interactions in flavoprotein catalysis. *Ann. N.Y. Acad. Sci.* **227**, 446-465
15. Thorpe, C., Matthews, R.G., and Williams, C.H., Jr. (1979) Acyl-coenzyme A dehydrogenase from pig kidney. Purification and properties. *Biochemistry* **18**, 331-337
16. Gorelick, R.J., Mizzer, J.P., and Thorpe, C. (1982) Purification and properties of electron-transferring protein from pig kidney. *Biochemistry* **21**, 6936-6942
17. Lau, S.-M., Powell, P., Buettner, H., Ghisla, S., and Thorpe, C. (1986) Medium-chain acyl coenzyme A dehydrogenase from pig kidney has instrinsic enoyl coenzyme A hydratase activity. *Biochemistry* **25**, 4184-4189

18. Hazekawa, I., Nishina, Y., Sato, K., Shichiri, M., and Shiga, K. (1995) Substrate activating mechanism of short-chain acyl-CoA, medium-chain acyl-CoA, long-chain acyl-CoA, and isovaleryl-CoA dehydrogenases from bovine liver: A resonance Raman study on the 3-ketoacyl-CoA complexes. *J. Biochem.* **118**, 900-910
19. Kawaguchi, A., Yoshimura, T., and Okuda, S. (1981) A new method for the preparation of acyl-CoA thioesters. *J. Biochem.* **89**, 337-339
20. Seubert, W., Lamberts, I., Kramer, R., and Ohly, B. (1968) On the mechanism of malonyl-CoA-independent fatty acid synthesis. I. The mechanism of elongation of long-chain fatty acids by acetyl-CoA. *Biochim. Biophys. Acta* **164**, 498-517
21. Thorpe, C. (1986) A method for the preparation of 3-ketoacyl-CoA derivatives. *Anal. Biochem.* **155**, 391-394
22. Stadtman, E.R. (1957) Preparation and assay of acyl coenzyme A and other thiol esters; Use of hydroxylamine in *Methods in Enzymology* (Colowick, S.P. and Kaplan, N.O., eds.) Vol. 3, pp. 931-941, Academic Press, New York
23. Sykes, P. (1981) *A Guidebook to Mechanism in Organic Chemistry*, 5th ed., pp. 204-206, Longman, London
24. Swoboda, B.E.P. and Massey, V. (1965) Purification and properties of the glucose oxidase from *Aspergillus niger*. *J. Biol. Chem.* **240**, 2209-2215
25. Williams, F.R. and Hager, L.P. (1966) Crystalline flavin pyruvate oxidase from *Escherichia coli*. I. Isolation and properties of the flavoprotein. *Arch. Biochem. Biophys.* **116**, 168-176
26. Massey, V. and Ganther, H. (1965) On the interpretation of the absorption spectra of flavoprotein with special reference to D-amino acid oxidase. *Biochemistry* **4**, 1161-1173
27. Powell, P.J., Lau, S.-M., Killian, D., and Thorpe, C. (1987) Interaction of acyl coenzyme A substrates and analogues with pig kidney medium-chain acyl-CoA dehydrogenase. *Biochemistry* **26**, 3704-3710
28. Kumar, N.R. and Srivastava, D.K. (1995) Facile and restricted pathways for the dissociation of octenoyl-CoA from the medium-chain acyl-CoA dehydrogenase (MCAD)-$FADH_2$-octenoyl-CoA charge-transfer complexes: Energetic and mechanism of suppression of the enzyme's oxidase activity. *Biochemistry* **34**, 9434-9443
29. Bowman, W.D. and Spiro, T.G. (1981) Normal mode analysis of lumiflavin and interpretation of resonance Raman spectra of flavoproteins. *Biochemistry* **20**, 3313-3318
30. Schmidt, J., Coudron, P., Thompson, A.W., Watters, K.L., and McFarland, J.T. (1983) Hydrogen bonding between flavin and protein: A resonance Raman study. *Biochemistry* **22**, 76-84
31. Lively, C.R. and McFarland, J.T. (1990) Assignment and the effect of hydrogen bonding on the vibrational normal modes of flavins and flavoproteins. *J. Phys. Chem.* **94**, 3980-3994
32. Nishina, Y., Sato, K., Shiga, K., Fujii, S., Kuroda, K., and Miura, R. (1992) Resonance Raman study on complexes of medium-chain acyl-CoA dehydrogenase. *J. Biochem.* **111**, 699-706
33. Miura, R., Nishina, Y., Fujii, S., and Shiga, K. (1996) ^{13}C-NMR study on the interaction of medium-chain acyl-CoA dehydrogenase with acetoacetyl-CoA. *J. Biochem.* **119**, 512-519
34. Thorpe, C. and Massey, V. (1983) Flavin analogue studies of pig kidney general acyl-CoA dehydrogenase. *Biochemistry* **22**, 2972-2978
35. Kim, J.-J.P., Wang, M., and Paschke, R. (1993) Crystal structures of medium-chain acyl-CoA dehydrogenase from pig liver mitochondria with and without substrate. *Proc. Natl. Acad. Sci. USA* **90**, 7523-7527
36. Zahler, W.L., Barden, R.E., and Cleland, W.W. (1968) Some physical properties of palmitoyl-coenzyme A micelles. *Biochim. Biophys. Acta* **164**, 1-11
37. Trievel, R.C., Wang, R., Anderson, V.E., and Thorpe, C. (1995) Role of the carbonyl group in thioester chain length recognition by the medium chain acyl-CoA dehydrogenase. *Biochemistry* **34**, 8597-8605
38. Lee, H.-J.,K., Wang, M., Paschke, R., Nandy, A., Ghisla, S., and Kim, J.-J.P. (1996) Crystal structures of the wild type and the Glu376Gly/Thr255Glu mutant of human medium-chain acyl-CoA dehydrogenase: Influence of the location of the catalytic base on substrate specificity. *Biochemistry* **35**, 12412-12420